

# Twin interaction with $\Sigma 11$ tilt grain boundaries in BCC Fe : Formation of new grain boundaries

G. Sainath<sup>a,\*</sup>, A. Nagesha<sup>a</sup>

<sup>a</sup>*Materials Development and Technology Division, Metallurgy and Materials Group, Indira Gandhi Centre for Atomic Research, HBNI, Kalpakkam, Tamilnadu-603102, India*

---

## Abstract

It is well known that the twinning is an important mode of plastic deformation in nanocrystalline materials. As a result, it is expected that the twin can interact with different grain boundaries (GBs) during the plastic deformation. Understanding these twin-GB interactions is crucial for our understanding of mechanical behavior of materials. In this work, the twin interaction with different  $\Sigma 11$  symmetric and asymmetric tilt GBs has been investigated in BCC Fe using molecular dynamics (MD) simulations. The results indicate that twin nucleate from the crack or GB and, its interaction with  $\Sigma 11$  asymmetric tilt GBs leads to the formation of a new GB. This new GB consist of  $\langle 100 \rangle$  Cottrell type immobile dislocations. The detailed atomistic mechanisms responsible for this new GB formation have been revealed using atomistic simulations. Interestingly, the new GB formation has not been observed in the case of twin interaction with  $\Sigma 11$  symmetric tilt GBs.

*Keywords:* BCC Fe; Twin; Grain Boundaries; Dislocations; Atomistic Simulations

---

## Highlights

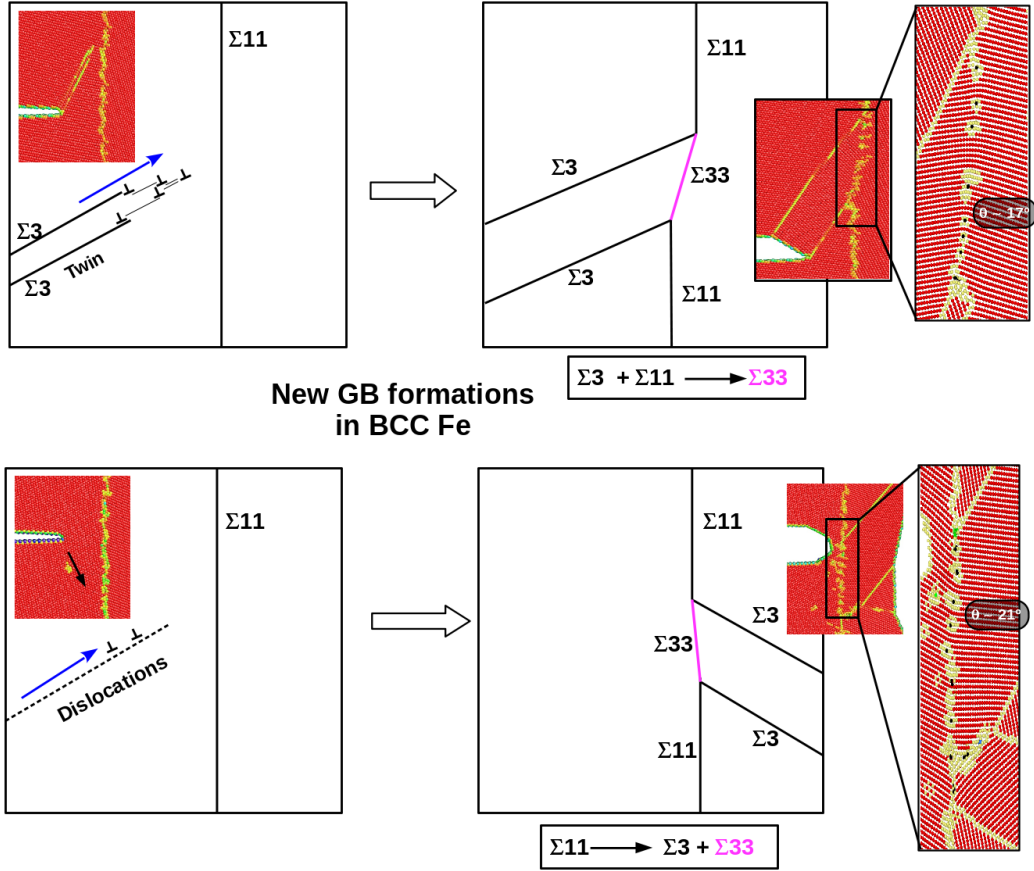
- In BCC Fe, interaction of twin with  $\Sigma 11$  ATGBs has been investigated using MD simulations.
- Twin interaction can transform the  $\Sigma 11$  ATGB into a new GBs consisting of  $[100]$  type immobile dislocations.
- The detailed atomistic mechanisms responsible for the new GB formations have been revealed.
- The new GB formation occurred according to  $\Sigma 3 + \Sigma 11 \rightarrow \Sigma 33$  and  $\Sigma 11 \rightarrow \Sigma 3 + \Sigma 33$  reactions.

---

\*Corresponding author

Email address: [sg@igcar.gov.in](mailto:sg@igcar.gov.in) (G. Sainath)

## Graphical Abstract



## 1. Introduction

Many structural materials are generally polycrystalline in nature and thus contain grain boundaries (GBs) with different structures and wide spectrum of energies [1, 2]. The structure and energy of the GBs determine the physical, chemical and mechanical properties of polycrystalline materials. Especially, the GBs play an important role in plastic deformation, radiation damage, corrosion resistance, crack propagation resistance and failure [1, 2, 3, 4, 5]. During the plastic deformation, the GBs interact with nearby grain boundaries, dislocations, twins, cracks, precipitates and many other defects. These defect interactions in turn lead to the grain/GB refinement, thus making the deformation more complex. As a result, investigating the defect-defect interactions through conventional experiments becomes difficult. In this context, the atomistic simulations can be utilized as an effective and efficient tool to examine the defect-defect interactions during the plastic deformation.

In the past many studies have been performed to understand the grain refinement through dislocation-GB interactions. For example, Koning et al. [6] have shown that the dislocation transmission across the  $\Sigma 11$  symmetric tilt GB results in local GB migration and disconnection formation in Ni. This process involves the

motion of GB dislocations, which are created due to the partial absorption of incoming dislocations. In a similar fashion, a twin boundary (TB) can transform itself into a curved GB due to the continuous impingement and accumulation of high density of dislocations [7]. This process occurs due to the rearrangement of densely arranged dislocations, which minimizes the strain energy. It has been shown that in nanocrystalline Pt, the glide of partial dislocations on two intersecting  $\{111\}$  planes transform the original  $\langle 110 \rangle \Sigma 3$  symmetric tilt GB into a  $\langle 110 \rangle \Sigma 9$  symmetric tilt high angle GB [8]. This TB transformation process has accommodated as large as 47% shear strain without initiating any cracks. In addition to dislocation-GB interactions, grain refinement via deformation twinning/de-twinning has also been reported. In duplex stainless steels, Cao et al. [9] have observed the formation of a new low angle GB or wall of dislocations due to the de-twinning of nanotwins. Similarly, the deformation twinning associated partial dislocation activity in Cu nanopillars has transformed the coherent TB into  $\Sigma 9$  boundary and also resulted in the formation of five-fold twin [10]. This transformation occurs when the edge of a micro twin approaches towards an already existing twin leading to the formation of  $\Sigma 9$  boundary at their intersection. The twin interaction with various twist and tilt GBs in HCP Mg has revealed that all the GBs were observed to have a blocking effect on deformation twinning and no new GB formation has been observed [11]. Apart from transforming the GB, the defect-GB interactions can also lead to annihilation of the GB itself. For example, the de-twinning in Cu and Fe nanopillars has led to the annihilation of TBs itself, thus making the twinned grains larger in size [12, 13]. Thus, it is important to characterize the dislocation-GB, twin-GB and crack-GB interactions in order to understand the grain refinement and GB engineering processes in materials.

However, most of these studies were focused on symmetric tilt GBs in FCC materials, even though the GBs in real polycrystalline materials are mostly asymmetric. Very few studies exist in BCC systems like Fe, which forms a basis for different structural materials of nuclear reactors. In BCC Fe, the twin interaction with  $\Sigma 3$  boundaries has been investigated using atomistic simulations [13]. It has been shown that the twin penetrates across the  $\Sigma 3$  boundary in two different ways; (1) it can penetrate directly to the next grain without any deviation in twinning plane and (2) it can pass onto a plane symmetrical to the original twinning plane. Further, this penetration has led the complete annihilation of pre-existing TBs [13]. However, in order to develop more reliable GB strengthening models, there is a need to study the twin interactions with many other grain boundaries like  $\Sigma 5$ ,  $\Sigma 9$ ,  $\Sigma 11$  etc. In view of this, the present study is focused on understanding the twin interaction with  $\Sigma 11$  symmetric and asymmetric tilt GBs in BCC Fe.

## 2. Simulation Methodology

### 2.1. Creation of grain boundaries

Molecular dynamics (MD) simulations have been carried out to study the interaction of a twin and crack with  $\Sigma 11$  symmetric and asymmetric tilt GBs in BCC Fe. Two different  $\Sigma 11$  symmetric and asymmetric tilt GBs have been considered in this study. These GBs have been created as follows; first, the  $\Sigma 11(332)$  symmetric tilt grain boundary (STGB) has been created by joining two separate grains, 1 and 2, with

crystallographic orientations as shown in Fig. 1a. This joining results in the formation of  $\Sigma 11(332)[1\bar{1}0]$  STGB with a misorientation angle ( $\theta$ ) of  $129.52^\circ$  at the interface (Fig. 1b). Following this, both grain 1 and 2, were rotated with an equal angle of  $\phi$ , known as GB inclination angle, around the  $[1\bar{1}0]$  axis (Figs. 1c,e,g). The rotation of grain 1 and 2 with an inclination angle ( $\phi$ ) =  $50.48^\circ$  as shown in Fig. 1c results in the formation of  $\Sigma 11(332)$  asymmetric tilt grain boundary (ATGB) with  $\theta = 129.52^\circ$  and  $\phi = 50.48^\circ$  at the interface (Fig. 1d). Similarly, the rotation with  $\phi = 90^\circ$  as shown in Fig. 1e leads to the formation of  $\Sigma 11(113)$  STGB with a misorientation angle ( $\theta$ ) =  $50.48^\circ$  at the interface (Fig. 1f). This boundary can also be represented as  $\Sigma 11(332)$  with  $\theta = 129.52^\circ$  and  $\phi = 90^\circ$ . Finally, the rotation with  $\phi = 129.52^\circ$  (Fig. 1g) results in the formation of  $\Sigma 11(332)$  ATGB with  $\theta = 129.52^\circ$  and  $\phi = 129.52^\circ$  at the interface (Fig. 1h). This boundary can also be represented as  $\Sigma 11(113)$  ATGB with  $\theta = 50.48^\circ$  and  $\phi = 50.48^\circ$  (Fig. 1h). This procedure of creating symmetric and asymmetric GBs is similar to that adopted in Ref.[14].

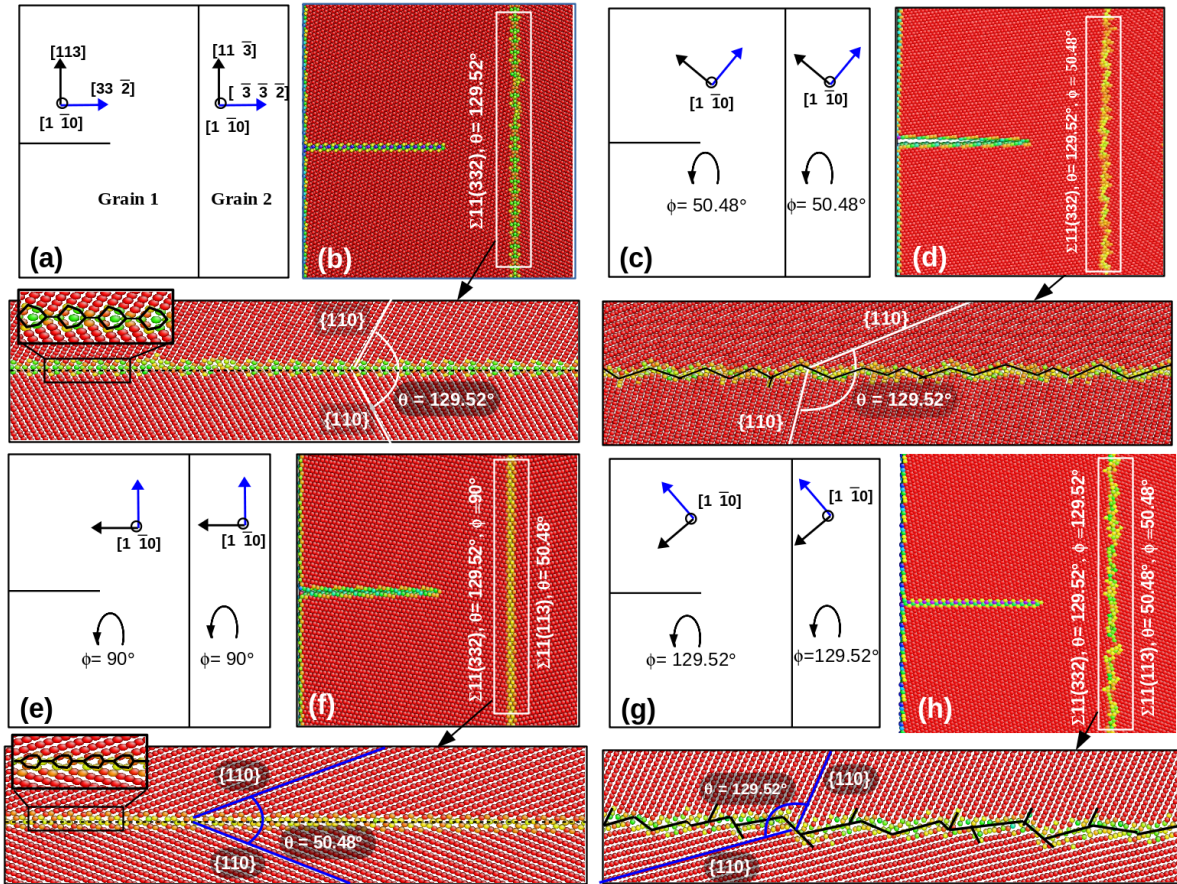


Figure 1: A schematic of the process of creating  $\Sigma 11$  symmetric and asymmetric tilt GBs along with their structures in BCC Fe. (a,b)  $\Sigma 11(332)$  STGB, (c,d)  $\Sigma 11(332)$  ATGB with  $\phi = 50.48^\circ$ , (e,f)  $\Sigma 11(113)$  STGB, and (g,h)  $\Sigma 11(332)$  ATGB with  $\phi = 129.52^\circ$  or  $\Sigma 11(113)$  ATGB with  $\phi = 50.48^\circ$ . The atoms in (b,d,f and h) are colored according to their centro-symmetry parameter (CSP) and visualized using AtomEye.



## 2.2. Structure of grain boundaries

The detailed analysis of the structure of the GBs indicated that the STGBs lie on single plane, (332) (Fig. 1b) and (113) (Fig. 1f) and these GB planes are inclined symmetrically with respect to {110} planes (Inset of Fig. 1b and f). Further, STGBs consist of periodically arranged structural units. On the contrary, ATGBs possess an asymmetric inclination with respect to the {110} planes and also the GB dissociates into small facets consisting of two different planes (Fig. 1d and h). This dissociation is in agreement with the fact that the ATGB would break up into small facets [15].

## 2.3. MD simulation details

In order to study the interaction of twin with  $\Sigma 11$  GBs, a sharp crack which acts as a twin or dislocation nucleation site has been introduced perpendicular to the GB plane (Fig. 1a-h). This sharp crack has been created by turning off the interactions between two slabs (groups) of atoms, i.e., by excluding the interactions between the fracture surfaces. This method effectively creates a crack between the two slabs without removing any atoms. The GB-crack system has a dimensions of  $17.37 \times 34.10 \times 1.61$  nm along  $x$ - $\langle 332 \rangle$ ,  $y$ - $\langle 113 \rangle$ , and  $z$ - $\langle 110 \rangle$  directions. The crack length was half the width of the specimen and the GB is placed at distance of 4.35 nm from the crack tip. Periodic boundary conditions were applied only in the crack front direction, i.e.,  $\langle 110 \rangle$ . On this model system, the mode-I loading has been simulated using MD simulations. All the simulations were carried out in LAMMPS package [16] employing the Mendeleev embedded atom method potential for BCC Fe [17]. Before loading, energy minimization was performed by conjugate gradient method to obtain a relaxed structure of the GB. Velocity verlet algorithm was used to integrate the equations of motion with a time step of 2 fs. Following energy minimization, the model system was equilibrated to a required temperature of 10 K in a canonical ensemble. Upon thermalization, the deformation was carried out in a displacement-controlled manner at constant strain rate of  $1 \times 10^8$  s $^{-1}$  by imposing displacements to atoms along the  $y$ -axis that varied linearly from zero at the bottom fixed layer to a maximum value at the top fixed layer. All the simulations were carried out till the strain reaches the value of 0.25. The stress was obtained using the Virial expression, which is equivalent to a Cauchy's stress in an average sense. AtomEye package [18] and OVITO [19] have been used for the visualization and dislocation analysis.

## 3. Results

### 3.1. Twin interaction with $\Sigma 11(332)$ $\phi = 50.48^\circ$ ATGB

Figure 2 shows the formation of a new GB due to the interaction of a twin (region enclosed by  $\Sigma 3(112)$  TBs) with  $\Sigma 11(332)$   $\phi = 50.48^\circ$  ATGB in BCC Fe. It can be seen that initially a twin embryo nucleates from the crack tip and approaches towards the ATGB (Fig. 2a). Once the twin front reaches the ATGB, its penetration and transmission to the neighboring grain is restricted (Fig. 2b). Following this, the width of the twin increases with increasing strain due to the continuous glide of twinning partials along the TBs (Fig.

2b-c). In this process of twin growth, the twinning partials interact with ATGB and transform the ATGB into a new GB as shown in Fig. 2c). This new GB consist of  $\langle 100 \rangle$  type immobile dislocations separated by a distance ( $d$ ) ranging from 0.68 to 1.25 nm. The misorientation angle ( $\theta$ ) across this boundary with respect to  $\langle 110 \rangle$  misorientation axis is found to be close to  $17^\circ$ , which makes it into the class of lower side of the medium angle GBs. It has also been found that the mean separation distance between the GB dislocations obeys the well-known Frank-Bilby equation [20], i.e.  $d = b/(2\sin(\theta/2))$ , where  $b$  is the Burgers vector of GB dislocations.

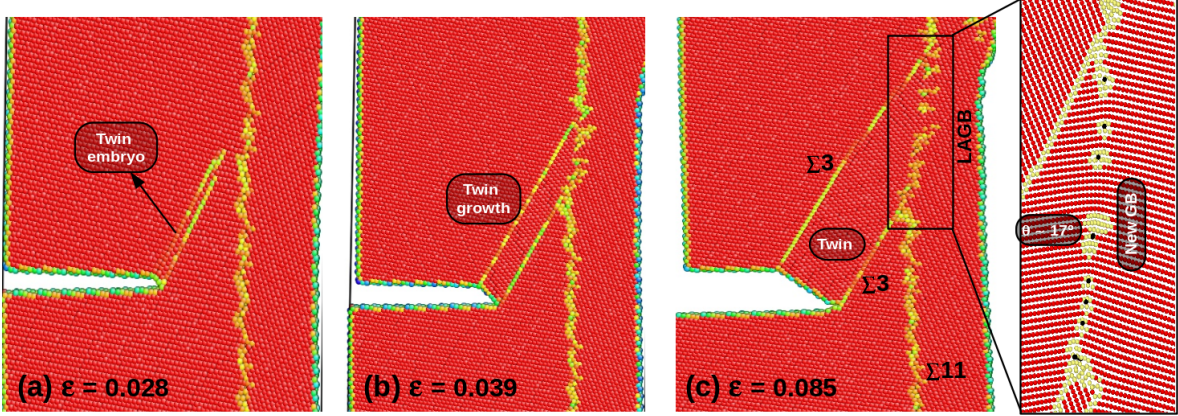


Figure 2: Formation of a new GB due to the interaction of a twin with  $\Sigma 11(332) \phi = 50.48^\circ$  ATGB in BCC Fe. (a) The twin nucleation from a crack tip, (b) twin growth, (c) a new GB formation at the interaction place of twin-ATGB. The atoms are colored according to their centro-symmetry parameter and visualized using AtomEye. The inset figure in (c) is visualized using OVITO. The black dots in inset of figure (c) are  $\langle 100 \rangle$  type dislocation lines.

Understanding the detailed mechanism responsible for such formation of a new GB is important in order to unravel the mechanism of grain refinement or reconfiguration of the GB network during the plastic deformation. Figure 3 shows the detailed atomistic and dislocation mechanisms responsible for the transformation of  $\Sigma 11$  ATGB into a new GB. It can be seen that the twin embryo nucleated from the crack tip consists of partial dislocations identified as 1,2 and 3 in Fig. 3a. With increasing strain, the twin front reaches the ATGB along with an increase in twin width and more partial dislocations, 4 and 5 (Fig. 3b). It can also be seen that the ATGB restrict the transmission of partial dislocations as well as twin into the next grain. Due to this restriction, the partial dislocations 1,2 and 3 pile-up and combine to form a  $1/2[111]$  full dislocation at the ATGB. This dislocation reaction can be written as

$$1/6[111] + 1/6[111] + 1/6[111] \longrightarrow 1/2[111]. \quad (1)$$

With further deformation, this full dislocation is emitted into the next grain by leaving a Cottrell dislocation [21] having a Burgers vector ( $b$ ) of  $[010]$  on the GB (Fig. 3c-d). This reaction can be written as

$$1/2[111] \longrightarrow [010] + 1/2[1\bar{1}1]. \quad (2)$$

Energetically, the above reaction is not feasible, i.e. violates the Frank criterion. However, the presence of high stresses within the GB make it feasible [22]. The same process described in Equation 1 and 2 occurs for the next set of partial dislocations 4,5 and 6 as shown in Fig. 3e-f. As a result, the emission of one more full dislocation can be seen in Fig. 3g and h. This emission of full dislocation leaves another Cottrell dislocation adjacent to the first one (Fig. 3h). With increasing strain, more and more Cottrell dislocations were added adjacent to each other (Fig. 3i-l). As a result, an increase in number of Cottrell dislocations from 3 in Fig. 3d (Magenta color lines) to 8 in Fig. 3l can be seen. These series of  $[100]$  Cottrell dislocations constitutes a new GB as shown in Fig. 2c. Thus, the interaction of a growing twin with an ATGB results in the formation of a new GB.

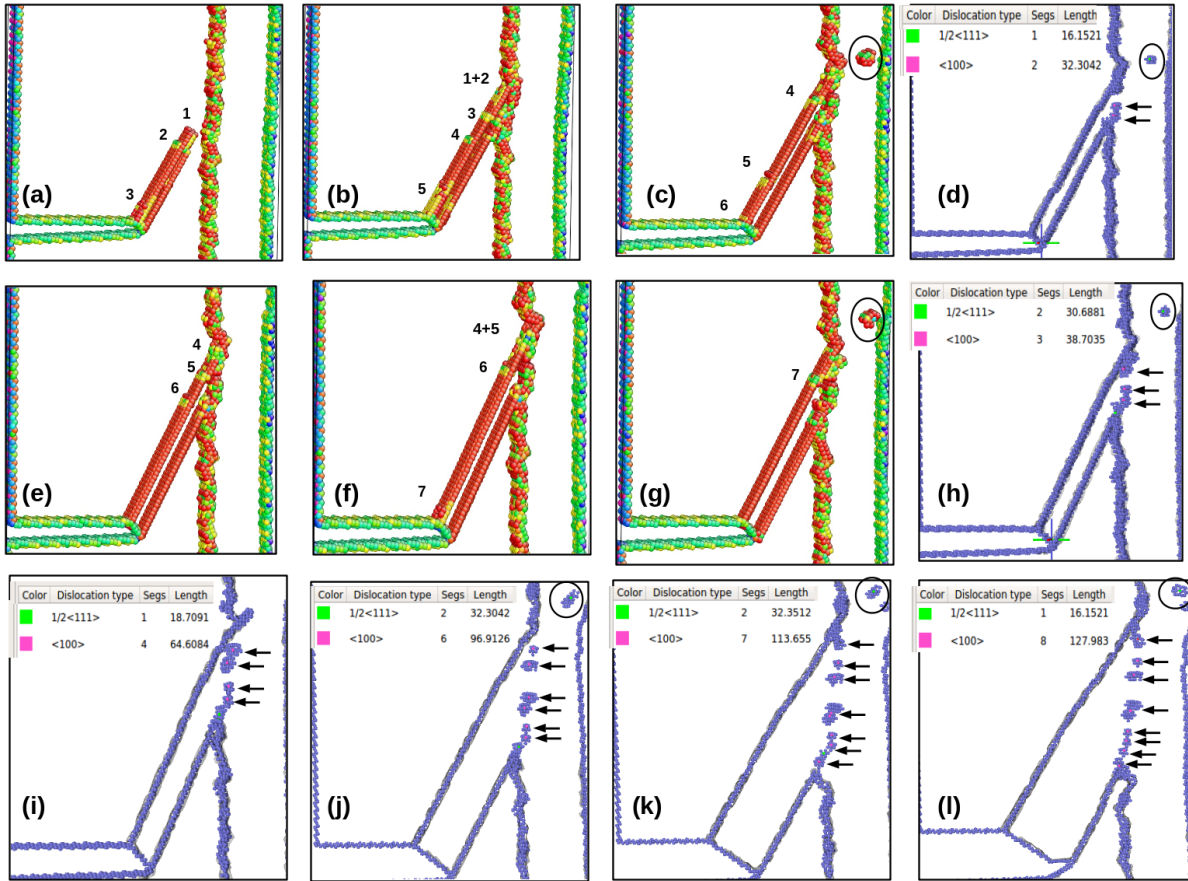


Figure 3: The detailed atomistic and dislocation mechanism responsible for the transformation of  $\Sigma 11(332)$   $\phi = 50.48^\circ$  ATGB into a new GB. The atoms in figure (a-c) and (e-g) are colored according to their centro-symmetry parameter and visualized using AtomEye. The atoms in figure (d) and (h-l) are colored according to their CNA parameter and visualized using OVITO. The inset tables show dislocation analysis results using OVITO. The magenta lines (dots in 2D) are  $\langle 100 \rangle$  type dislocations, while the green lines are  $1/2\langle 111 \rangle$  type dislocations. The numbers 1,2,...,7, represent the partial dislocations gliding on twin boundaries. For clarity, the  $\langle 100 \rangle$  type dislocations (pink dots) were also shown with black arrow marks.

### 3.2. Twin interaction with $\Sigma 11(113)$ $\phi = 50.48^\circ$ ATGB

Figure 4 shows the formation of a new GB due to the interaction of a dislocation and twin with  $\Sigma 11(113)$   $\phi = 50.48^\circ$  ATGB. It can be seen that, at first, a dislocation nucleates from the crack tip and glide towards



the ATGB (Fig. 4a). Once the dislocation reaches close to the boundary, it triggers the nucleation of twin from the ATGB into the neighboring grain (Fig. 4b). With increasing strain, more dislocations nucleate from the crack tip along with an increase in twin width (Fig. 4c). Following this, one more twin nucleate from the ATGB and grow on a twin plane different from the original one (Fig. 4c-d). At this stage, the dislocations also start nucleating from the ATGB-twin junction into the first/left grain as shown in Fig. 4e. The continuous growth of both the twins has led to the formation of a new GBs as shown in Fig. 4f and inset. The careful examination of the newly formed GB has indicated that it consist of a series of  $\langle 100 \rangle$  type immobile dislocations separated by a distance (d) ranging from 0.6 to 1.0 nm and the misorientation angle ( $\theta$ )  $\sim 21^\circ$  (lower side of the medium angle GBs) with respect to the  $\langle 110 \rangle$  misorientation axis. Also, the mean distance between the GB dislocations obeys Frank-Bilby equation [20].

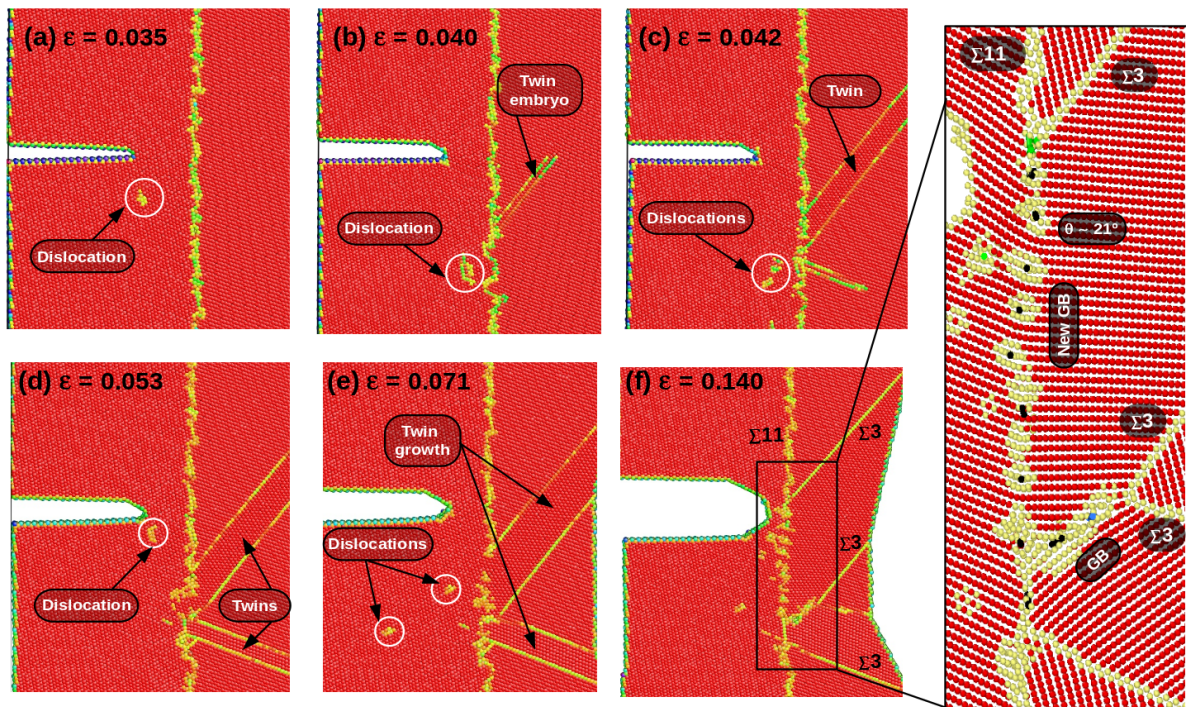


Figure 4: Formation of a new GB due to the interaction of a dislocation/twin with  $\Sigma_{11}(113)$   $\phi = 50.48^\circ$  ATGB in BCC Fe. (a) Dislocation nucleation from a crack tip, (b) nucleation of a twin from the GB due to dislocation-GB interaction, (c-d) twin growth along with new twin nucleation, (e) dislocation nucleation from the GB-twin junction back into the first/left grain, and (f) twin growth and new GB formation. The atoms are colored according to their centro-symmetry parameter and visualized using AtomEye. The inset figure in (f) is visualized using OVITO. The black dots in inset of figure (f) are  $\langle 100 \rangle$  type dislocation lines.

Figure 5 shows the detailed mechanisms responsible for the formation of a new GB in Fig. 4. It has been observed that, following twin formation, the subsequent nucleation of dislocations from the crack tip is mainly responsible for both adding dislocations to new GB and also aiding the twin growth. The series of snapshots in Figure 5a show a mechanism where a dislocation nucleated from the crack tip is reflected by the  $\Sigma_{11}(113)$  GB back into to the same grain by leaving a Cottrell dislocation [21] with a Burgers vector of

[100] on the GB. This reaction can be written as



Here,  $1/2[\bar{1}11]$  is the dislocation nucleated from the crack tip,  $[100]$  is the Cottrell type GB dislocation and  $1/2[\bar{1}\bar{1}\bar{1}]$  is the dislocation reflected back by the ATGB into the original grain (Fig. 5a). Different from this, the snapshots in Fig. 5b shows another mechanism, where a dislocation nucleated from the crack tip ( $1/2[\bar{1}11]$ ) interacts with the reflected dislocation from the earlier reaction (Eq. 3), and form a  $[100]$  type Cottrell dislocation slightly away from the GB according to the following reaction;



Eventually, this  $[100]$  dislocation is attracted and readjusted into the GB (Fig. 5b). These mechanisms shown in Fig. 5a-b occur multiple times leading to the addition of many  $[100]$  type dislocations to the new GB.

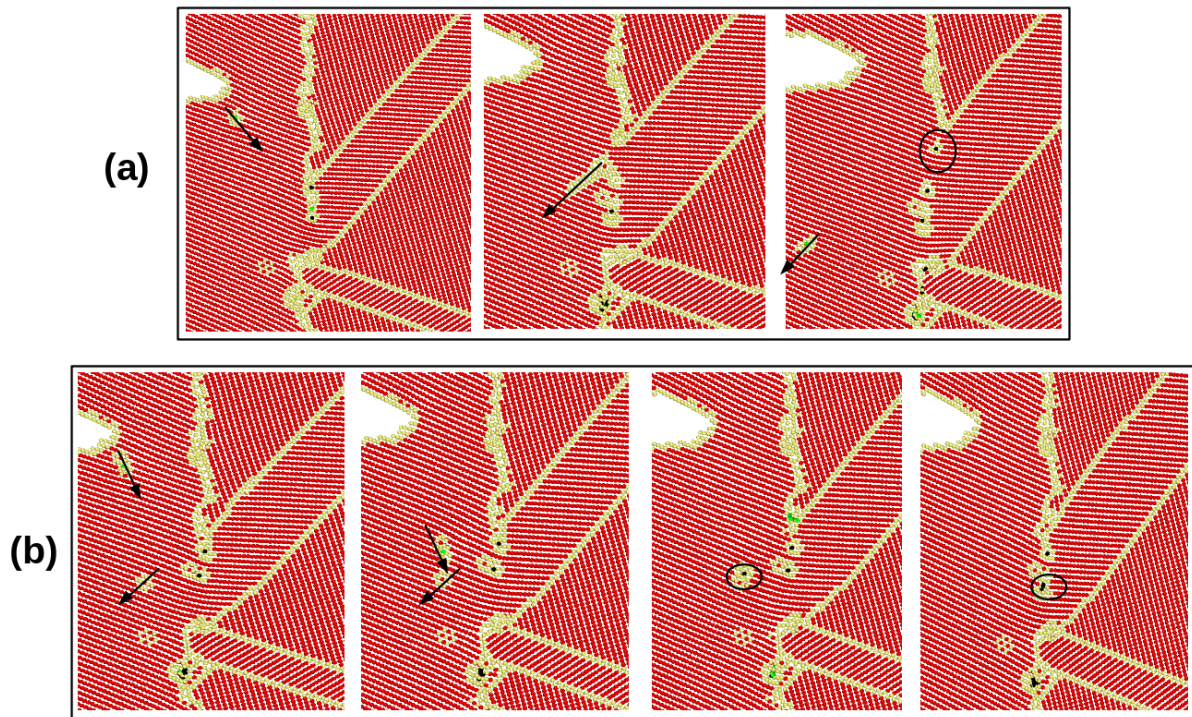


Figure 5: The detailed atomistic and dislocation mechanism responsible for the transformation of  $\Sigma 11(113) \phi = 50.48^\circ$  ATGB into a new GB. Series of snapshots in (a) details a mechanism, where a dislocation nucleated from the crack tip is reflected by ATGB back into to the same grain by leaving a  $[100]$  dislocation on the new GB. Series of snapshots in (b) manifest a mechanism, where a dislocation nucleated from the crack tip interacts with the reflected dislocation and form a  $[100]$  type Cottrell dislocation slightly away from the boundary, which eventually attracted towards the new GB.



### 3.3. Crack interaction with $\Sigma 11(332)$ and $\Sigma 11(113)$ STGBs

Similar to ATGBs, the crack growth behavior in the presence of  $\Sigma 11(332)$  and  $\Sigma 11(113)$  STGBs has also been investigated and presented in Fig. 6. It can be seen that the crack in case of  $\Sigma 11(332)$  STGB grows in a brittle manner on  $\{110\}$  plane without any micro-twin at the crack tip (Fig. 6a). Once the crack tip reaches the GB, the crack gets blunted due to the emission of dislocations (Fig. 6b-d). With increasing strain, more and more dislocations emit from the crack-GB intersection leading to significant crack blunting. On the other hand, the crack in presence of  $\Sigma 11(113)$  STGB emits a twin embryo (Fig. 6A), which becomes a full twin once it reaches the GB (Fig. 6B). Subsequently, the twin interacts with  $\Sigma 11(113)$  STGB and its transmission into the next grain is restricted. As a result, the STGB near the interaction site is distorted from its original plane. With increasing strain, a new twin nucleates from the distorted GB (Fig. 6C-D). Further deformation has led to the growth of this newly formed twin without forming any new GB. These results indicate that in case of  $\Sigma 11$  STGBs neither the transformation nor the formation of any new GB occurs. Similar results were observed in the case of  $\Sigma 3$  STGB in BCC Fe [5], where the brittle crack transmit to next grain without changing the structure of the GB. These results on  $\Sigma 11$  and  $\Sigma 3$  boundaries suggest that the STGBs are stable against the plastic deformation.

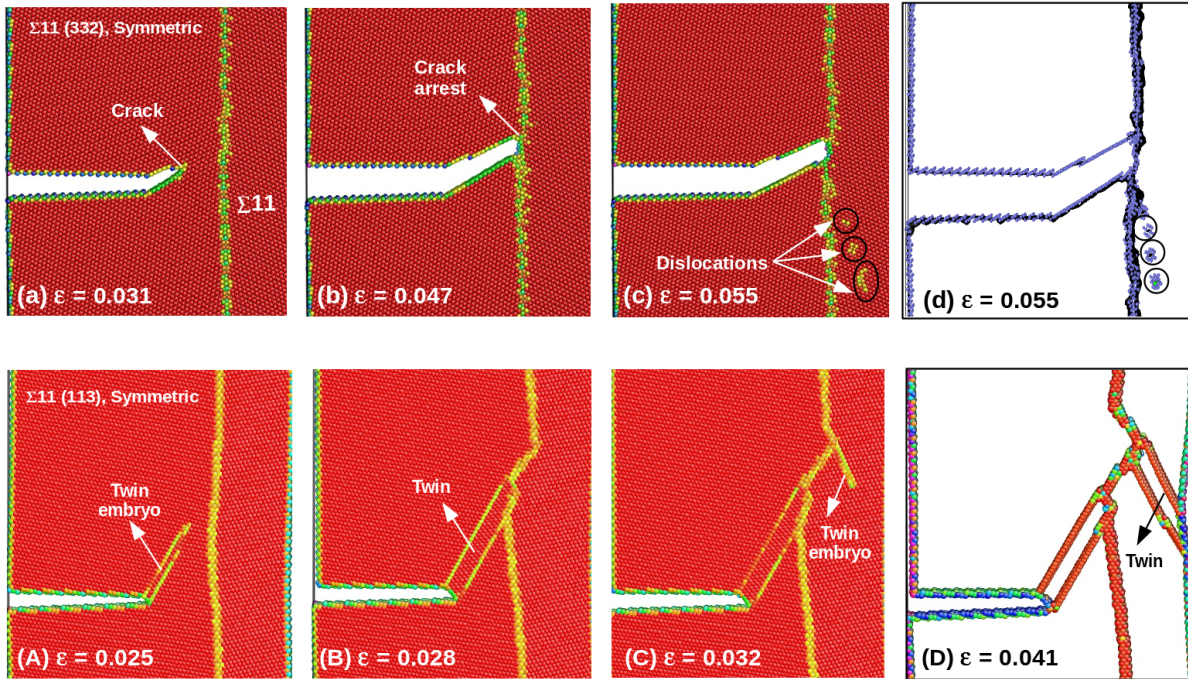


Figure 6: The crack growth behavior in presence of (a-d)  $\Sigma 11(332)$  STGB, and (A-D)  $\Sigma 11(113)$  STGB in BCC Fe. In (a-d) once the brittle crack reaches the GB, the crack gets blunted significantly due to the emission of multiple dislocations from the GB and no transformation of GB is seen. In (A-D) twin nucleates from the crack tip and once it reaches the GB, its transmission to the next grain is restricted leading to the distortion of STGB without any transformation. The atoms in (a-c) and (A-D) are colored according to their centro-symmetry parameter and visualized using AtomEye. The atoms in figure (d) are colored according to their CNA parameter and visualized using OVITO.

#### 4. Discussion

The present results suggest that the twin interaction with  $\Sigma 11$  ATGBs lead to the formation of a new GBs. These new GBs have misorientation angle of  $17^\circ$  and  $21^\circ$ , which falls in the lower side of the medium angle GB spectrum. Since these boundaries also consist of a well separated dislocations, they can be considered as low angle GBs. Accordingly, the new GBs observed in the present investigation are classified as low angle GBs. The generally accepted misorientation angle for transition from low to high angle GBs is in the range of  $10 - 20^\circ$ , depending on the material, misorientation axis, GB normal etc. [23]. The low angle GBs form when multiple dislocations rearrange themselves into configurations of lower energy during the plastic deformation [24]. However, the low angle GB formation due to the interaction of a twin with ATGB as observed in the present investigation is interesting. The low angle GBs consisting of Cottrell type immobile dislocations have important consequences in mechanical properties, grain refinement processes, GB engineering and deformation behavior of materials. It is known that the low angle boundaries have lower GB energies than regular high angle boundaries and accordingly, they contribute to the thermal stability of microstructures and hence improve the mechanical properties of polycrystalline materials [25]. The low angle GBs also act as strong and tunable barriers (tunable barrier allows the transmission of only selective dislocations based on the orientation relationship) for dislocation motion, thus contributing to hardening as well as softening of materials[26].

In GB engineering, it is established that the twinning alters and modifies mainly the  $\Sigma 3$  and its higher order boundaries i.e.,  $\Sigma 9$  and  $\Sigma 27$ , through the well known reaction

$$\Sigma 3 + \Sigma 3 \longrightarrow \Sigma 3^n, \quad (5)$$

where n is an integer[3]. However, the present results indicate that the twin can also alter the other high angle GBs like  $\Sigma 11$  and contribute to the formation of new GBs. As schematically shown in Fig. 7, a possible reactions for this new GB formation can be written as [3, 27]

$$\Sigma 3 + \Sigma 11 \longrightarrow \Sigma 33 \quad (\text{Figure 7a}) \quad (6)$$

and

$$\Sigma 11 \longrightarrow \Sigma 3 + \Sigma 33 \quad (\text{Figure 7b}). \quad (7)$$

Here, the  $\Sigma 33$  GB generally has a misorientation angle ( $\theta$ ) =  $20.1^\circ$  with respect to  $\langle 110 \rangle$  misorientation axis [28]. Interestingly, the misorientation angles of new GBs observed in the present investigation are  $\theta \sim 17^\circ$  and  $21^\circ$  with respect to the  $\langle 110 \rangle$  axis, which are close to misorientation angle of  $\Sigma 33$  GB. This suggest that the new GB observed in the present study is approximately  $\Sigma 33$  and its formation occurs due to the interaction of twin with  $\Sigma 11$  ATGB according to the Eqs. 6 and 7. These kind of GB transformations

strongly influence the structure and associated properties of many polycrystalline materials [25]. However, the transformation of GBs has not been observed in the case of symmetric  $\Sigma 11$  GBs, indicating that the symmetric boundaries are stable against the GB transformations during the plastic deformation.

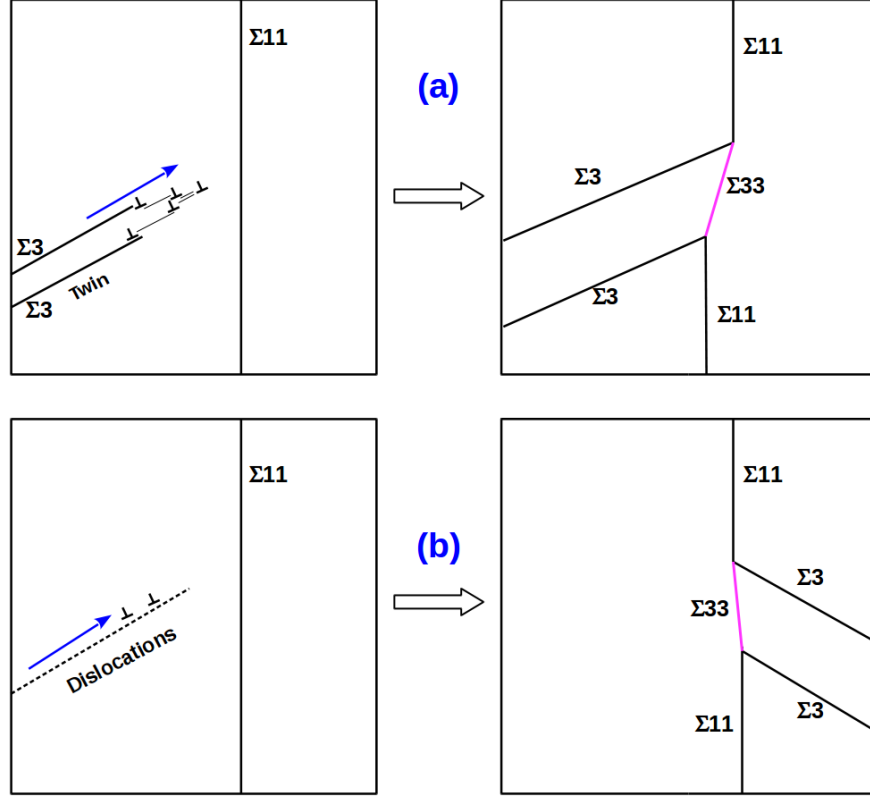


Figure 7: A schematic of twin-ATGB interactions observed in the present study. (a) GB interactions observed in the case of  $\Sigma 11(332)$   $\phi = 50.48^\circ$  ATGB ( $\Sigma 3 + \Sigma 11 \rightarrow \Sigma 33$ ), and (b) GB interactions observed in the case of  $\Sigma 11(113)$   $\phi = 50.48^\circ$  ATGB ( $\Sigma 11 \rightarrow \Sigma 3 + \Sigma 33$ ).

## 5. Conclusions

The interaction of a twin with  $\Sigma 11$  symmetric and asymmetric tilt GBs has been investigated in BCC Fe using atomistic simulations. The results indicated that the growing twin can transform the  $\Sigma 11$  ATGBs into a new GBs consisting of  $[100]$  type immobile dislocations. This transformation has occurred through a systematic activity of partial  $(1/6\langle 111 \rangle)$  and full  $(1/2\langle 111 \rangle)$  dislocations. The  $\Sigma 11(332)$   $\phi = 50.48^\circ$  ATGB restrict the penetration and transmission of a twin and twinning partials into the neighboring grain. Due to this restriction, the twinning partials  $(1/6\langle 111 \rangle)$  gliding on the TBs pile-up and combine to form a  $1/2[111]$  full dislocation at the  $\Sigma 11(332)$  ATGB. With further deformation, this  $1/2[111]$  full dislocation is emitted into the next grain by leaving a  $[100]$  Cottrell type dislocations on the GB. The same process occurs repeatedly leaving a series of  $[100]$  type immobile dislocations constituting a new GB. In case of  $\Sigma 11(113)$   $\phi = 50.48^\circ$  ATGB, once the dislocation nucleated from the crack tip reaches close to the boundary, it

triggers the nucleation of twin from the boundary into the neighboring grain. Following twin formation, the subsequent nucleation of dislocations from the crack tip is mainly responsible for both adding dislocations to new GB and also aiding the twin growth. However, these kind of transformations or new GB formations have not been observed in the case of twin interaction with  $\Sigma 11$  symmetric boundaries.

The misorientation angles of newly formed GBs in the present investigation are close to misorientation angle of  $\Sigma 33$  GB. This suggested that the new GB formation in the present study occurred according to  $\Sigma 3 + \Sigma 11 \rightarrow \Sigma 33$  and  $\Sigma 11 \rightarrow \Sigma 3 + \Sigma 33$  reactions. Thus, the present study sheds a light on the transformation mechanism of ATGB into new GBs due to deformation twinning and it has important consequences in grain refinement processes, grain boundary engineering and deformation behavior of materials.

### Data availability

The data that support the findings in this paper are available from the corresponding author on request.

### References

### References

- [1] V. Randle, Grain boundary engineering: an overview after 25 years, *Mater. Sci. Tech.* 26 (2010) 253-261.
- [2] T. Watanabe, Grain boundary engineering: historical perspective and future prospects, *J. Mater. Sci.* 46 (2011) 4095-4115.
- [3] V. Randle, Twinning-related grain boundary engineering, *Acta Mater.* 52 (2004) 4067-4081.
- [4] X. Xiao, H. Chu, H. Duan, Effect of grain boundary on the mechanical behaviors of irradiated metals: a review, *Sci. China-Phys. Mech. Astron.* 59 (2016) 664601.
- [5] G. Sainath, A. Nagesha, Atomistic simulations of twin boundary effect on the crack growth behaviour in BCC Fe, *Trans. Ind. Nat. Acad. Eng.* (2021) 1-7.
- [6] M. de Koning, R.J. Kurtz, V.V. Bulatov, C.H. Henager, R.G. Hoagland, W. Cai, M. Nomura, Modeling of dislocation-grain boundary interactions in FCC metals, *J. Nucl. Mater.* 323 (2003) 281-289.
- [7] N.R. Tao, K. Lu, Nanoscale structural refinement via deformation twinning in face-centered cubic metals, *Scr. Mater.* 60 (2009) 1039-1043.
- [8] L. Wang, T. Jiao, W. Yu, S. Xuechao, X. Sisi, M. Shengcheng, Y. Guanghua, Z. Zec, Z. Jind, H. Xiaodong, In situ atomic scale mechanisms of strain-induced twin boundary shear to high angle grain boundary in nanocrystalline Pt, *Ultramicroscopy* 195 (2018) 69-73.

- [9] Y. Cao, Y.B. Wang, X.H. An, X.Z. Liao, M. Kawasaki, S.P. Ringer, T.G. Langdon, Y.T. Zhu, Grain boundary formation by remnant dislocations from the de-twinning of thin nano-twins, *Scr. Mater.* 100 (2015) 98-101.
- [10] G. Sainath, Sunil Goyal, A. Nagesha, Atomistic mechanisms of twin-twin interactions in Cu nanopillars, *Comput. Mater. Sci.* 185 (2020) 109950.
- [11] J. Tang, H. Fan, D. Wei, W. Jiang, Q. Wang, X. Tian, X. Zhang, Interaction between a  $\{10\bar{1}2\}$  twin boundary and grain boundaries in magnesium, *Inter. J. Plast.* 126 (2020) 102613.
- [12] G. Cheng, S. Yin, T.-H. Chang, G. Richter, H. Gao, Y. Zhu, Anomalous tensile detwinning in twinned nanowires. *Phys. Rev. Lett.* 119 (2017) 256101.
- [13] G. Sainath, Sunil Goyal, A. Nagesha, Plasticity through de-twinning in twinned BCC nanowires, *Crystals* 10 (2020) 366.
- [14] X.J. Long, L. Wang, B. Li, J. Zhu, S.N. Luo, Shock-induced migration of  $\Sigma 3\langle 110 \rangle$  grain boundaries in Cu, *J. Appl. Phys.* 121 (2017) 045904.
- [15] D.L. Medlin, K. Hattar, J.A. Zimmerman, F. Abdeljawad, S.M. Foiles, Defect character at grain boundary facet junctions: Analysis of an asymmetric  $\Sigma 5$  grain boundary in Fe, *Acta Mater.* 124 (2017) 383-396.
- [16] S. Plimpton, Fast parallel algorithms for short-range molecular dynamics, *J. Comp. Phys.* 117 (1995) 1-19.
- [17] M.I. Mendeleev, S. Han, D.J. Srolovitz, G.J. Ackland, D.Y. Sun, M. Asta, Development of new interatomic potentials appropriate for crystalline and liquid iron, *Philos. Mag.* 83 (2003) 3977-3994.
- [18] J. Li, AtomEye: an efficient atomistic configuration viewer, *Modell. Simul. Mater. Sci. Eng.* 11 (2003) 173-177.
- [19] A. Stukowski, Visualization and analysis of atomistic simulation data with OVITO-the Open Visualization Tool, *Modell. Simul. Mater. Sci. Eng.* 18 (2010) 015012.
- [20] A.P. Sutton, R.W. Balluffi, *Interfaces in Crystalline Materials*, Oxford University Press, 1995.
- [21] A.H. Cottrell, Theory of brittle fracture in steel and similar metals, *Trans. Met. Soc. AIME* 212 (1958) 196.
- [22] Y. Guo, D.M. Collins, E. Tarleton, F. Hofmann, J. Tischler, W. Liu, R. Xu, A.J. Wilkinson, T.B. Britton, Measurements of stress fields near a grain boundary: Exploring blocked arrays of dislocations in 3D, *Acta Mater.* 96 (2015) 229-236.



- [23] M. Winning, A.D. Rollett, Transition between low and high angle grain boundaries, *Acta Mater.* 53 (2005) 2901-2907.
- [24] G. E. Dieter, *Mechanical metallurgy*, McGraw-hill, New-York, 1976.
- [25] S.V. Bobylev, M. Yu. Gutkin, I.A. Ovid'ko, Transformations of grain boundaries in deformed nanocrystalline materials, *Acta Mater.* 52 (2004) 3793-3805.
- [26] S. Chen, Q. Yu, The role of low angle grain boundary in deformation of titanium and its size effect, *Scripta Mater.* 163 (2019) 148-151.
- [27] J. Humphreys and M. Hatherly, *Recrystallization and related annealing phenomena*, Elsevier, (1996) Page 217.
- [28] D. Scheiber, R. Pippan, P. Puschnig, L. Romaner, Ab initio calculations of grain boundaries in bcc metals, *Modelling Simul. Mater. Sci. Eng.* 24 (2016) 035013.